Type-I interferon signaling through ISGF3 complex is required for sustained Rip3 activation and necroptosis in macrophages

Scott McComb[a,b,1], Erin Cessford[a,1], Norah A. Alturki[a], Julie Joseph[a], Bojan Shutinoski[a], Justyna B. Startek[a,c], Ana M. Gamero[d], Karen L. Mossman[e], and Subash Sad[a,2]

[a]Department of Biochemistry, Microbiology and Immunology, Faculty of Medicine, University of Ottawa, Ottawa, ON, Canada K1N 6N5; [b]Department of Oncology, University Children's Hospital, University of Zurich, 8032 Zürich, Switzerland; [c]Department of Cellular and Molecular Medicine, Katholieke Universiteit Leuven, 3000 Leuven, Belgium; [d]Department of Biochemistry, Temple University School of Medicine, Philadelphia, PA 19140; and [e]Department of Pathology and Molecular Medicine, McMaster University, ON Canada L8S 4L8

Edited by Vishva M. Dixit, Genentech, San Francisco, CA, and approved June 27, 2014 (received for review April 17, 2014)

Myeloid cells play a critical role in perpetuating inflammation during various chronic diseases. Recently the death of macrophages through programmed necrosis (necroptosis) has emerged as an important mechanism in inflammation and pathology. We evaluated the mechanisms that lead to the induction of necrotic cell death in macrophages. Our results indicate that type I IFN (IFN-I) signaling is a predominant mechanism of necroptosis, because macrophages deficient in IFN-α receptor type I (IFNAR1) are highly resistant to necroptosis after stimulation with LPS, polyinosinic-polycytidylic acid, TNF-α, or IFN-β in the presence of caspase inhibitors. IFN-I–induced necroptosis occurred through both mechanisms dependent on and independent of Toll/IL-1 receptor domain-containing adaptor inducing IFN-β (TRIF) and led to persistent phosphorylation of receptor-interacting protein 3 (Rip3) kinase, which resulted in potent necroptosis. Although various IFN-regulatory factors (IRFs) facilitated the induction of necroptosis in response to IFN−β, IRF-9–STAT1– or -STAT2–deficient macrophages were highly resistant to necroptosis. Our results indicate that IFN-β–induced necroptosis of macrophages proceeds through tonic IFN-stimulated gene factor 3 (ISGF3) signaling, which leads to persistent expression of STAT1, STAT2, and IRF9. Induction of IFNAR1/Rip3–dependent necroptosis also resulted in potent inflammatory pathology in vivo. These results reveal how IFN-I mediates acute inflammation through macrophage necroptosis.

Innate immune cells, such as macrophages, serve as one of the first lines of defense against invading pathogens. Upon recognition of pathogen-associated molecular patterns (PAMPs) such as bacterial LPS, macrophages are activated to initiate inflammation through the release of cytokines (1). Recently it has been demonstrated that, when combined with caspase inhibition, LPS also can initiate a form of programmed necrotic cell death (necroptosis) that is dependent on signaling through the receptor-interacting proteins 1 and 3 (Rip1 and Rip3) (2). These results add to the number of cell-stress pathways shown to stimulate necroptotic signaling, including cell death receptor signaling (3), secondary mitochondria-derived activator of caspases mimetics (4), viral infection (5), and genotoxic stress (6).

Recent work has demonstrated convincingly that activation of the Rip1 and Rip3 kinases is associated with the release of potent inflammatory cytokines even in the absence of cell death (7, 8). Consistent with this association, necrostatin-1, an inhibitor of Rip1 kinase activity, has been demonstrated to block Rip1-dependent activation of TNF-α production (9). Downstream of necrotic cell death, the release of intracellular damage-associated molecular patterns (DAMPs) into the extracellular environment has been thought to promote the inflammatory phenotype associated with this form of cell death (10). Various reports have demonstrated that deficiency in necroptosis signaling in vivo leads to less inflammatory pathology in mouse models of systemic inflammatory shock (11–13).

Macrophages recognize PAMPs through Toll-like receptors (TLRs). The LPS receptor TLR4 activates two distinct signaling axes: the myeloid differentiation response gene-88 dependent pathway (Myd88), which leads to NF-κB activation (14), and the Toll/interleukin-1 receptor domain-containing adapter-inducing IFN-β (TRIF) dependent pathway, which leads to the production of type I interferons (IFN-I) (15). Recently TRIF also has been directly implicated in the induction of necroptotic signaling (2, 16). The IFN-I receptor is composed of a heterodimer of the two IFN-α receptor type I proteins (IFNAR1 and IFNAR2). Binding of IFN-I (IFN-α or IFN-β) to the ubiquitous IFN-I receptor (IFNAR1) activates several signaling pathways, including JAK/STAT, NF-κB, and PI3K (17). The best-studied IFN-I signaling pathway involves the activation of the Janus kinases JAK1 and Tyk2, which in turn activate STAT1 and induce an antiviral state within the cell. STAT1 activates the expression of genes which encode proteins such as protein kinase R (PKR), which shuts down protein translation, and IFN-regulatory factor 9 (IRF9), which further modifies the gene response to IFN (18). In the presence of IRF9 expression, IFN signaling leads to the formation of the STAT1/STAT2/IRF9 complex known as "ISGF3," which acts as a powerful antiviral regulatory complex within the cell (19). Given the wide clinical relevance of IFN-I in conditions ranging from hepatitis C infection (20), to cancer (21), multiple

Significance

Although it has long been known that inflammatory immune responses are associated with death of cells through necrosis, the mechanisms controlling this process are not yet well understood. Recently a type of programmed inflammatory cell death, necroptosis, has been discovered. In this paper we reveal previously unidentified molecular mechanisms that operate to induce this form of cell death. Our results indicate that in order to undergo necroptosis, immune cells must produce and receive signals from the key immune regulator, interferon. Such interferon-dependent necroptosis of immune cells drives acute inflammatory pathology in a mouse model of sepsis. This work highlights the intimate connection between cell death and inflammation, and may lead to new understanding and treatment of inflammatory pathologies.

Author contributions: S.S. designed research; S.M., E.C., N.A.A., J.J., B.S., and J.B.S. performed research; A.M.G., K.L.M., and S.S. contributed new reagents/analytic tools; S.M., E.C., and S.S. analyzed data; and S.M., E.C., and S.S. wrote the paper.

The authors declare no conflict of interest.

This article is a PNAS Direct Submission.

[1]S.M. and E.C. contributed equally to this work.

[2]To whom correspondence should be addressed. Email: subash.sad@uottawa.ca.

This article contains supporting information online at www.pnas.org/lookup/suppl/doi:10.1073/pnas.1407068111/-/DCSupplemental.

sclerosis (22), atherosclerosis (23), and diabetes (24), novel insight into mechanisms of IFN-I is highly relevant to the understanding and treatment of these diseases.

In this paper we provide evidence that IFN-I signaling is necessary for sustained Rip3 activation and the induction of necroptosis after LPS, polyinosinic-polycytidylic acid (polyI:C), or TNF-α stimulation of macrophages. Specifically, we show that ISGF3-dependent IFNAR1 signaling results in sustained activation of Rip3. Finally, we show that IFN-induced necroptosis drives systemic inflammatory shock. Thus, we have provided a mechanism for the central role of IFN-I in necroptosis and acute inflammatory shock (25–27). The ability of IFN-I to induce inflammatory necroptosis in innate immune cells represents a paradigm shift in the understanding of both necroptosis and IFN-I.

Results

IFN-I Signaling Is Required for LPS-Induced Necroptosis in Macrophages. Most studies on necroptosis involve evaluation of the signaling mechanisms in nonimmune cells (28), in which case necroptosis most commonly is induced by stimulating cells with TNF-α in the absence of caspase signaling (benzyloxycarbonyl-Val-Ala-Asp-fluoromethylketone, zVAD-FMK) (29). Our results obtained with similar experimental protocols indicate that mouse embryonic fibroblasts undergo necroptosis in response to TNF-α but not LPS signaling (Fig. 1*A*). Interestingly, bone marrow-derived macrophages undergo necroptosis in response to both TNF-α and LPS in combination with zVAD (Fig. 1*A*). Cell death was evaluated relative to respective treatment controls (LPS, IFN-β, or TNF-α) in the absence of zVAD. When cells were treated with cytokines or PAMPs alone, no cell death was noticeable (Fig. S1 *A* and *B*). Induction of cell death also was rescued completely by necrostatin-1 (a specific inhibitor of Rip1 kinase activity), thus confirming the cell death pathway to be necroptosis (Fig. 1*A*). We find that this induction of cell death occurs 8–24 h after treatment (Fig. S1 *C* and *D*). Although there is a dose-dependent increase in necroptosis when zVAD is combined with LPS, treatment of macrophages with zVAD alone or with LPS alone does not lead to necroptosis (Fig. 1*B*). Having noted that macrophages, unlike fibroblasts, displayed unique susceptibility to necroptosis in response to LPS, we were interested in dissecting the mechanism of necroptosis induction in this important cell type. We also observed that LPS/zVAD-induced cell death of macrophages was dependent on the expression of Rip3 kinase (Fig. 1*C*) and was independent of TNF signaling (Fig. 1*D*). Although TNF-α is considered to be a canonical inducer of necroptosis (29), our results indicate that this is not the case for macrophages.

To decipher the mechanism through which LPS signaling induced necroptosis of macrophages, we next examined macrophages deficient for key signaling mediators. We observed that TRIF-deficient macrophages were resistant to zVAD/LPS-induced death, but Myd88-deficient macrophages were not protected (Fig. 1*E*). Because TRIF signaling is involved primarily in the production of IFN-I in response to TLR stimulation (15), we tested whether IFNAR1 signaling might be important in the induction of LPS-induced necroptosis. Indeed, we found that IFNAR1-deficient macrophages were highly resistant to necroptosis induced by LPS/zVAD (Fig. 1 *F* and *G*). These results indicate that IFNAR1 signaling is necessary for the induction of necroptosis of macrophages after LPS stimulation.

IFNAR1 Signaling Is Vital for Necroptosis Induced by Multiple Pathways in Macrophages. Similar to our observations in LPS, IFNAR1- and Rip3-deficient but not TNF receptor 1 (TNFR1)- and TNFR2-deficient macrophages showed resistance to necroptosis induction when TLR3 was engaged through polyI:C stimulation (Fig. 2 *A–C*). Surprisingly, even with the canonical inducer of necroptosis, TNF-α, we found that both IFNAR1 and Rip3 expression are needed for induction of necroptotic cell death (Fig. 2 *D–F*). Furthermore, IFN-β treatment resulted in necroptosis of TNFR-deficient macrophages (Fig. 2*G*) but failed to do so in IFNAR1- or Rip3-deficient macrophages (Fig. 2 *G–I*). These results indicate that IFNAR1 signaling, rather than

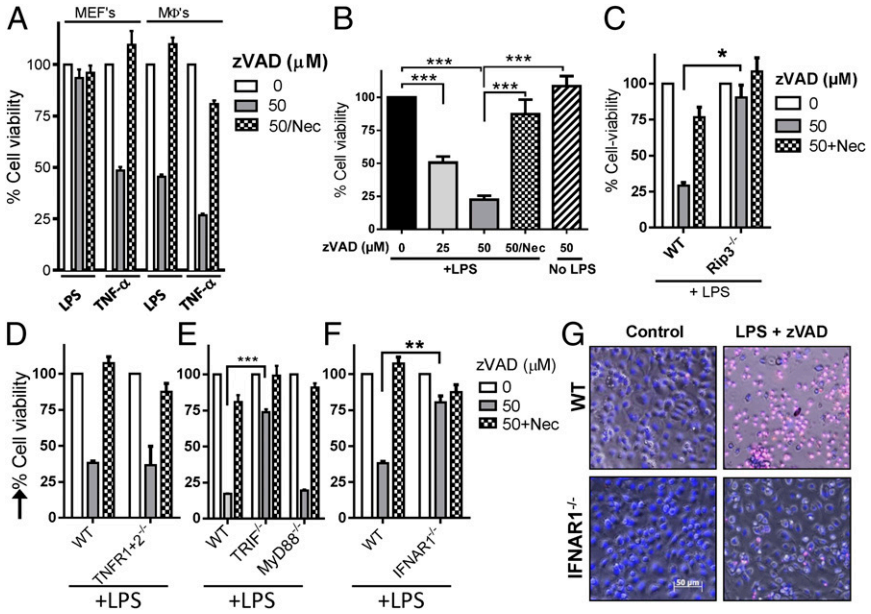

Fig. 1. IFN-I is required for LPS-induced necroptosis in macrophages. (*A*) Bone marrow-derived macrophages and mouse embryonic fibroblasts were treated with LPS (100 ng/mL), TNF-α (50 ng/mL), zVAD (50 μM), and/or necrostatin-1 (30 μM) as shown. After 24 h, cells were examined for viability via the MTT assay. (*B–F*) Macrophages generated from bone marrow obtained from various knockout mice were treated for 24 h with various combinations of LPS, zVAD (25–50 μM), and necrostatin-1 (30 μM) and were examined for viability using the MTT assay. Graphs show the percentage of viable cells ± SEM relative to cells treated with the corresponding stimuli in the absence of zVAD from at least three repeated experiments performed in triplicate. *$P < 0.05$; **$P < 0.001$; ***$P < 0.0001$. (*G*) Macrophages generated from WT or IFNAR1-deficient bone marrow were treated as described above and were examined for viability using Hoechst and propidium iodide costaining.

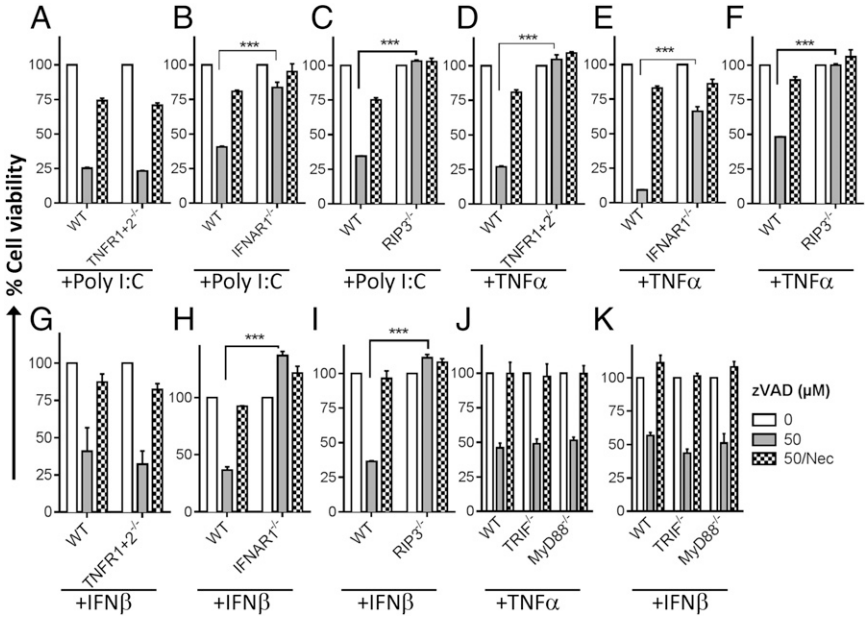

Fig. 2. IFNAR1 signaling is necessary for poly:I:C-, TNF-, and IFN-I–dependent necroptosis. (*A*–*K*) Macrophages generated from bone marrow obtained from various knockout mice were treated for 24 h with various combinations of LPS, zVAD (25–50 μM), and necrostatin-1 (30 μM) as indicated and examined for viability using the MTT assay. Graphs show the percentage of viable cells ± SEM relative to cells treated with the corresponding stimuli in the absence of zVAD from at least three biological replicate experiments performed in duplicate. Statistical analysis was performed only to compare the effect of +zVAD treatment on different genotypes (gray bars). ***$P < 0.0001$.

TNF-α signaling, is a predominant mechanism of necroptosis in macrophages. Interestingly, both TRIF- and Myd88-deficient macrophages showed no resistance to TNF-α– or IFN-β–induced necroptosis (Fig. 2 *J* and *K*). These results emphasize that necroptosis in macrophages can be induced through diverse pathways that are always dependent on IFNAR1 signaling.

IFNAR1 Signaling Sustains Prolonged Activation of Rip3. Rip1 and Rip3 activation (phosphorylation) can be measured via SDS/PAGE through a shift in migration of these proteins (4, 30). Treatment of WT macrophages with LPS resulted in phosphorylation of Rip1 but not Rip3 kinase (Fig. 3*A*, lane 2). In contrast to Rip1 activation, LPS induced phosphorylation of Rip3 only when the cells also were treated with zVAD (Fig. 3*A*, lane 3). Treatment with zVAD alone did not result in significant phosphorylation of Rip1 or Rip3 (Fig. S2*A*). As expected, necrostatin-1 also was able to block Rip1-dependent phosphorylation of Rip3 completely but had no effect on Rip1 phosphorylation (Fig. 3*A*, lane 4). We also observed that

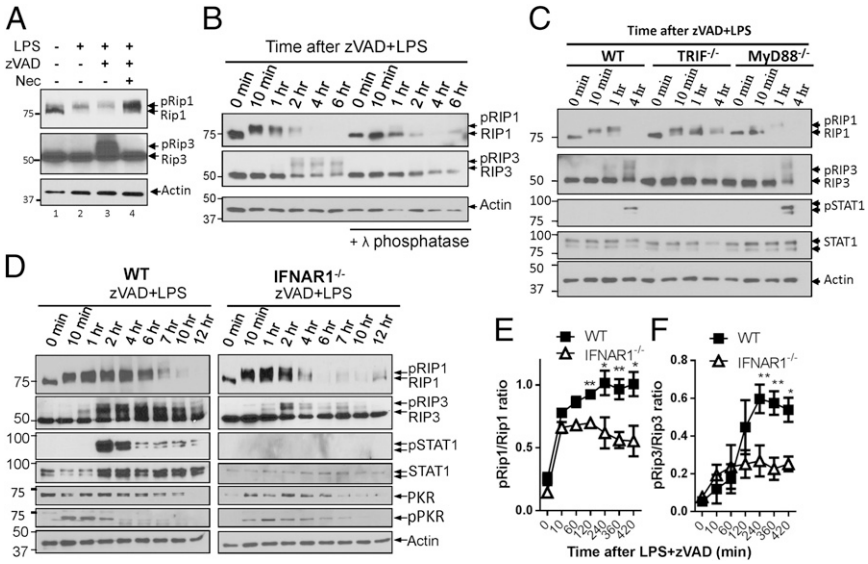

Fig. 3. IFNAR1 signaling sustains prolonged activation of Rip3. (*A*) Macrophages generated as described in *Experimental Procedures* were treated for 2 h with various combinations of LPS, zVAD (50 μM), and necrostatin-1 (30 μM) as shown. Lysates then were examined by Western blot. (*B*–*D*) Macrophages generated from various knockout mouse strains were treated with zVAD (50 μM) and LPS for varying time intervals as shown. Lysates then were examined by Western blot. (*E* and *F*) Densitometry was performed to quantitate the average ratio of pRip1/total Rip1 and pRip3/total Rip3 ± SEM over at least three separate experiments performed as described above.

Rip3 phosphorylation occurred later than Rip1 activation, beginning at 2 h and being maintained until at least 6 h posttreatment (Fig. 3*B*). We confirmed that these slower-migrating forms of Rip1 and Rip3 were indeed phosphorylated, because treatment of lysates with lambda phosphatase eliminated the upper bands (Fig. 3*B*, *Right*). We were not able to detect phosphorylation of mixed lineage kinase domain-like protein (MLKL) using a similar technique (Fig. S2*B*). These results indicate that induction of necroptosis by LPS/zVAD leads to rapid phosphorylation of Rip1 that is followed by delayed activation of Rip3.

At 4 h posttreatment with LPS/zVAD, phosphorylation of Rip3 was strongly attenuated in TRIF-deficient macrophages, in contrast to Myd88-deficient and WT macrophages (Fig. 3*C*). Longer time courses confirm that phosphorylation of Rip3 occurs between 2 and 6 h posttreatment in WT and Myd88-deficient cells but is attenuated in TRIF-deficient macrophages (Fig. S2*C*). Interestingly, phosphorylation of Rip1 kinase seems to be slightly delayed in Myd88-deficient macrophages (Fig. 3*C* and Fig. S2*C*). These data suggest that both the Myd88- and TRIF-dependent pathways may be implicated in the activation of Rip1 and Rip3 phosphorylation.

As in TRIF-deficient cells, in the absence of IFNAR1 expression we observed only a transient induction of Rip3 activation after LPS/zVAD treatment (Fig. 3*D*). Interestingly, we also saw an IFN-I–dependent increase in STAT1 phosphorylation coinciding with the activation of Rip3 kinase (Fig. 3*D*).This increase in STAT1 and Rip3 phosphorylation coincided with the induction of IFN-I release and preceded cell death as defined by loss of plasma membrane integrity (Fig. S1). Densitometric analysis of repeated Western blots revealed that the ratio of phosphorylated to unphosphorylated Rip1 was slightly lower in IFNAR1-deficient macrophages at later time points (Fig. 3*E*). Analysis also confirms the more significant differences in Rip3 phosphorylation in WT and IFNAR1-deficient cells (Fig. 3*F*). Importantly, densitometric analysis showed no difference in the loss of total Rip1 during necroptosis in WT or IFNAR1-deficient macrophages, and we observed no difference in the induction of Rip1 transcription (Fig. S2 *D* and *E*). These data show that autocrine IFN-I signaling functions to sustain pronecroptotic Rip1 and Rip3 phosphorylation long enough to allow the induction of necroptosis.

IRF9 Expression Is Required for Sustained Rip3 Activation and Necroptosis. A key family of transcription factors, IRFs, promotes the production of IFN and modifies signal transduction after IFNAR1 engagement. Interestingly, in our model we observed a partial rescue from necroptosis in macrophages lacking IRF3 but only a minor rescue in those lacking IRF7 (Fig. 4*A* and Fig. S3 *A* and *B*). In addition we observed a partial rescue in macrophages deficient in IRF1 (Fig. 4*B*). Interestingly, IRF1 was particularly important for TNF-α– but not IFN-β–induced necroptosis (Fig. S3 *C* and *D*). Although most IRFs promote the production of IFN by the host cell, IRF9 plays a unique role in facilitating the downstream response to IFN-I (19). In contrast to the partial rescues we observed with IRF1-, IRF3-, and IRF7-knockout macrophages, IRF9 macrophages were highly resistant to the induction of necroptosis by LPS, IFN-β, and TNF-α (Fig. 4 *C*–*E*). Interestingly, we observed a partial rescue of polyI:C-induced necroptosis in IRF9-deficient macrophages (Fig. 4*F*). In our time-course Western blots we also observed a lack of late Rip3 activation in cells lacking IRF9 expression (Fig. 4 *G*–*I*) similar to that in IFNAR1-deficient cells. Overall these results indicate that IRFs act redundantly to facilitate the induction of IFN-I in response to LPS, but IRF9 is specifically required for the induction of necroptotic cell death.

The ISGF3 Complex Promotes Necroptotic Cell Death. We next were interested in dissecting the mechanism downstream of IFN signaling that might promote necroptosis of macrophages. Previous work has suggested that PKR promotes the phosphorylation of Rip1 and Rip3 (2). In contrast to this result, we find that PKR-deficient macrophages show no resistance to necroptosis (Fig. S4*A*). It should be noted that PKR-deficient macrophages were generated on a 129SvJ background mouse strain, although we confirmed a similar requirement of IFNAR1 for necroptosis in macrophages on a 129 genotype (Fig. S4*B*). These results indicate that PKR is not essential for IFN-I–dependent necroptosis in macrophages.

Given the necroptotic role for IRF9 that we have demonstrated here and IRF9 mediation of signal transduction through the ISGF3 complex (31), we hypothesized that IFN-I might mediate necroptosis specifically through the ISGF3 complex. ISGF3,

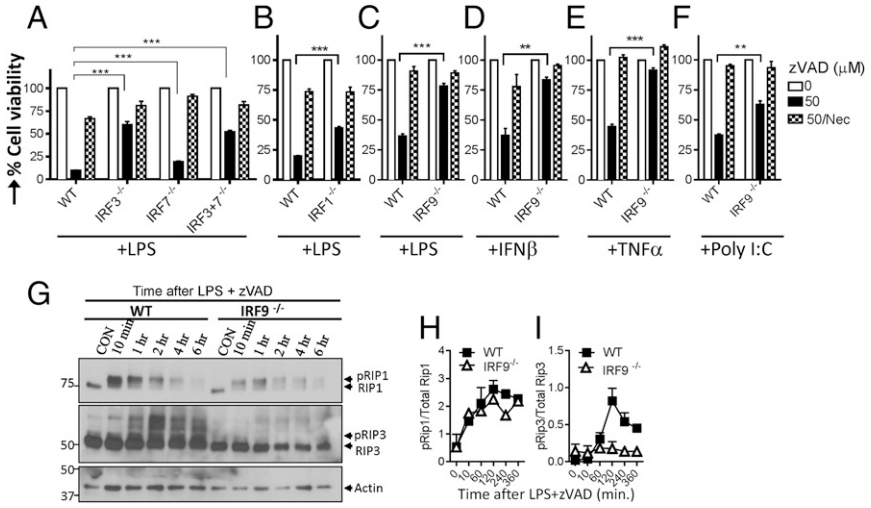

Fig. 4. IRF9 expression is required for sustained Rip3 activation and necroptosis. (*A*–*F*) Macrophages generated from bone marrow obtained from various knockout mice were treated for 24 h with various combinations of LPS, zVAD (25–50 μM), and necrostatin-1 (30 μM) and were examined for viability using the MTT assay. Graphs show the percentage of viable cells ± SEM relative to cells treated with the corresponding stimuli in the absence of zVAD ± SEM from at least three repeated experiments performed in triplicate. $^{**}P < 0.001$; $^{***}P < 0.0001$. (*G*) Macrophages derived from the bone marrow of WT or IRF9$^{-/-}$ mice were treated for varying time intervals with LPS and zVAD as shown. Lysates then were examined via Western blot. (*H* and *I*) Densitometry was performed to quantitate the average ratio of pRip1 to pRip3 over at least three separate experiments performed as described above.

consisting of a complex of IRF9, STAT1, and STAT2, migrates to the nucleus to induce transcription of specific target genes (32). Consistent with a pronecroptotic role for ISGF3, we observed that STAT1-deficient macrophages were partially resistant to necroptosis induced by IFN-β, TNF-α, polyI:C, or LPS (Fig. 5 *A–D*). We also observed that macrophages lacking STAT1 showed reduced Rip3 phosphorylation in response to LPS/zVAD (Fig. 5*E*). Similarly, STAT2-deficient macrophages were resistant to necroptosis induced by IFN-β, TNF-α, polyI:C, or LPS (Fig. 5 *F–I*) and showed lower levels of Rip3 phosphorylation after LPS/zVAD treatment (Fig. 5*J*). These data implicate the key members of the ISGF3 complex—IRF9, STAT1, and STAT2—in the induction of necroptotic cell death.

Low-level constitutive IFN has been thought to induce tonic signaling that promotes the activation of STAT1 and STAT2 (32). Consistent with this notion, we observed that IFNAR1-deficient macrophages express very low levels of constitutive STAT1 and STAT2, and these levels remained very low even after stimulation with LPS/zVAD (Fig. 5*K*). Furthermore, IFNAR1-deficient macrophages displayed greatly reduced IRF9 transcript levels with no induction after LPS+zVAD stimulation (Fig. 5*L*), pinpointing ISGF3 as a critical promoter of necroptosis. Stimulation of WT macrophages with IFN-β alone resulted in a gradual increase in the expression of STAT1 and STAT2, consistent with the timing of necroptotic cell death (Fig. 5*M*). Overall these results support the conclusion that IFN-activated induction of the ISGF3 complex is required for the activation of necroptosis within macrophages.

IFN-I–Mediated Necroptosis Drives Inflammatory Pathology in Vivo. Several recent reports have highlighted the role of IFN-I in acute systemic inflammation (25, 27, 33); therefore we wanted to investigate the effects of IFN-I–dependent necroptosis specifically in vivo. To test the role of IFN-I, we injected WT and IFNAR1-deficient mice with LPS and zVAD. After an injection of a very low dose of LPS (2.5 mg/kg) and zVAD (5 mg/kg), IFNAR1-deficient mice showed a significantly smaller drop in body temperature than WT mice (Fig. 6*A*). Rip3-knockout mice showed a similarly reduced response to a low dose of LPS/zVAD in vivo (Fig. 6*A*). At a time point when WT mice were almost moribund (slow movement and hunched posture), IFNAR1-deficient mice appeared relatively normal (Movie S1).

Next, we examined the inflammatory cytokine levels in mice at 18 h postinjection of LPS/zVAD. In this case, we observed that IFNAR1-deficient mice showed lower levels of inflammatory cytokines in their serum (Fig. 6*B*). We observed a similar trend of lower cytokine expression in Rip3-deficient mice (Fig. S5). We also observed that after injection of LPS/zVAD IFNAR1-deficient mice showed higher numbers of macrophages and significantly lower cell death within the macrophage population (Fig. 6*C*). These data clearly show that IFN-I signaling is a key element in the induction of inflammatory necroptosis in vivo.

Finally, we wanted to confirm that differences in the IFN-I–induced necroptosis pathway could affect mouse survival. After the injection of a higher dose of LPS/zVAD, mice showed early signs of distress, including a rapid drop in body temperature. WT mice reached the humane endpoint of severe pathology and body temperature below 27 °C within 6–10 h (Fig. 6*D*). In contrast, both IFNAR1-deficient and Rip3-deficient mice showed a slower

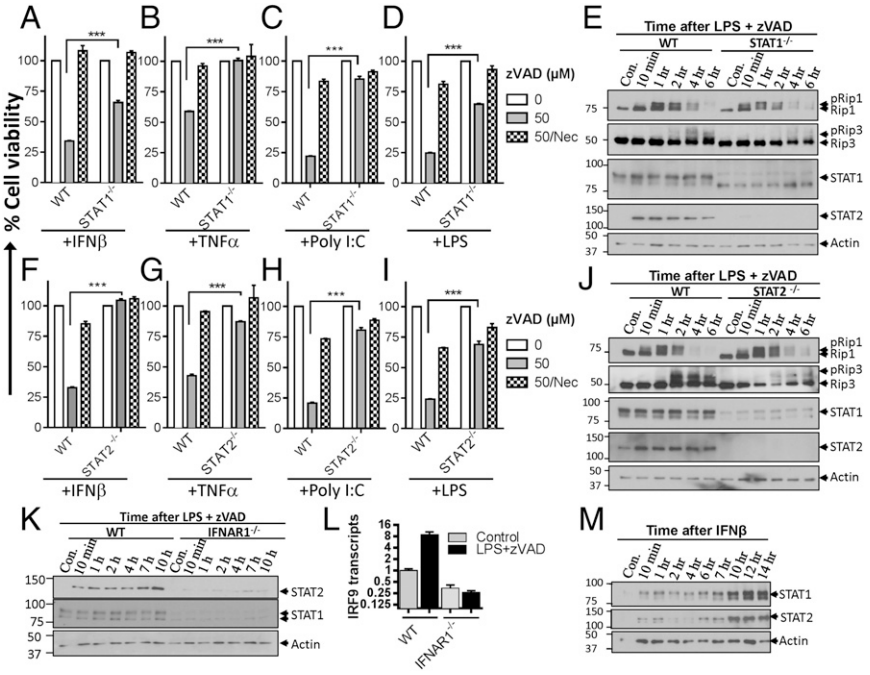

Fig. 5. The ISGF3 complex promotes necroptotic cell death. (*A–D*) Macrophages generated from bone marrow obtained from STAT1-knockout and matching WT mice were treated for 24 h with various combinations of LPS, TNFα, polyI:C, zVAD (50 μM), and necrostatin-1 (30 μM) as shown and were examined for viability using the MTT assay. (*E*) Macrophages derived from the bone marrow of WT, STAT1$^{-/-}$, or IFNAR1$^{-/-}$ mice were treated for varying time intervals with LPS and zVAD as shown. Lysates then were examined via Western blot. (*F–J*) Macrophages from STAT2-knockout and WT mice were generated and treated as described above. Graphs show the percentage of viable cells ± SEM relative to cells treated with the corresponding stimuli in the absence of zVAD from at least three repeated experiments performed in triplicate. Statistical analysis was performed only to compare the effect of +zVAD treatment on different genotypes (gray bars). ***$P < 0.0001$. (*K*) Macrophages generated from WT and IFNAR1$^{-/-}$ mice were treated for varying time intervals with LPS and zVAD (50 μM) and were examined for the expression of STAT1 and STAT2 by Western blot. (*L*) Total RNA for quantitative RT-PCR was extracted from WT and IFNAR1$^{-/-}$ bone marrow-derived macrophages after 6 h with or without LPS + zVAD treatment. (*M*) WT macrophages were cultured with IFN-β (100 U/mL) for various time intervals, and cell extracts were tested for the expression of STAT1 and STAT2 by Western blotting.

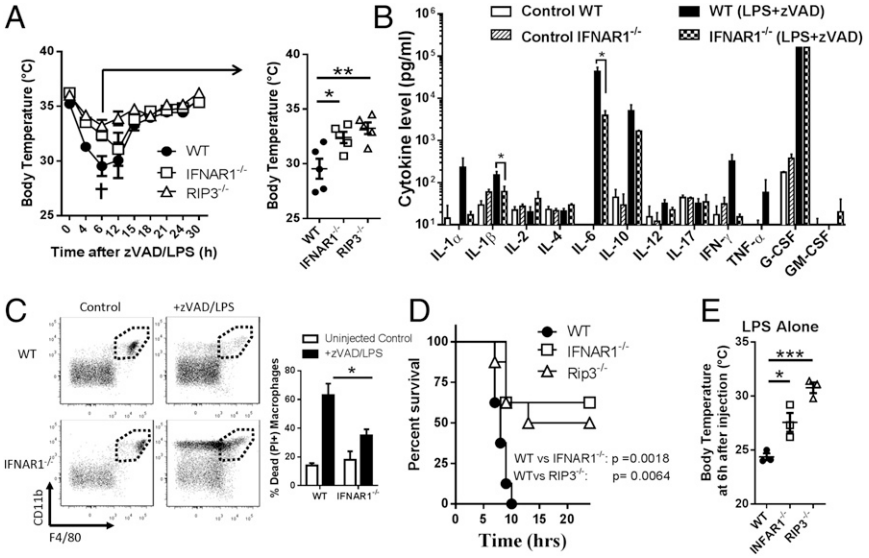

Fig. 6. In vivo injection of LPS/zVAD leads to IFNAR1/Rip3-dependent necroptosis and inflammatory pathology. (*A*) (*Left*) WT, IFNAR1$^{-/-}$, and Rip3$^{-/-}$ mice were injected with a low dose of LPS (2.5 mg/kg) and zVAD (5 mg/kg) and were monitored for a drop in body temperature. (*Right*) Spread of body temperature at 6 h postinjection ($n = 5$ mice per group). (*B*) WT and IFNAR1$^{-/-}$ mice were challenged with a higher dose of LPS (5 mg/kg) and zVAD (5 mg/kg) and were killed at 18 h postinjection. Serum was drawn by cardiac puncture and was examined for cytokine levels via ELISA array ($n = 3$ mice per group). (*C*) After cardiac puncture, peritoneal lavage was performed and examined via flow cytometric analysis ($n = 3$ mice per group). (*D*) WT, IFNAR1$^{-/-}$, and Rip3$^{-/-}$ mice were challenged with a lethal dose of LPS (10 mg/kg) and zVAD (5 mg/kg) and were examined for survival over 24 h ($n = 8$ WT and 5 IFNAR1/Rip3 genotypes). (*E*) WT, IFNAR1$^{-/-}$, and Rip3$^{-/-}$ mice were challenged with a lethal dose of LPS alone (50 mg/kg) and were examined for body temperature 6 h after challenge ($n = 3$ mice per group). All graphs show mean measurements ± SEM. $^{*}P < 0.05$; $^{**}P < 0.001$;$^{***}P < 0.0001$.

progression of pathology, and 50–60% of mice remained healthy beyond 24 h (Fig. 6*D*). Finally, we examined the drop in body temperature of mice injected with a lethal dose of LPS in the absence of zVAD (50 mg/kg). Again we observed a significant difference between WT and Rip3-deficient or IFNAR1-deficient mice (Fig. 6*E*). These data support a model in which IFN-I–induced necroptosis is a significant driver of inflammatory pathology and may play a key role in acute inflammatory pathology such as observed in sepsis.

Discussion

The understanding of programmed necrotic cell death has advanced rapidly in recent years. It is now known that various immunostimulatory and cell-stress pathways converge to stimulate the phosphorylation-induced formation of the Rip1/Rip3 necrosome complex (10, 34). Previously, it was thought that strong inducers of necroptosis such as TNF-α/zVAD or LPS/zVAD rely primarily on the direct activation of Rip1 phosphorylation through specific signaling complexes (2, 35). In contrast to this view, however, our evidence indicates that feedback signaling through IFNAR1 is necessary for the sustained Rip1 and Rip3 activation which leads to necroptotic cell death (Fig. 7).

Our work establishes that Rip1 kinase is activated quickly in response to TLR stimulation. For Rip1 activation, we find that caspase inhibition is irrelevant and serves only to prevent the later induction of Rip3 phosphorylation. This result adds to previous work showing that caspase-8 promotes the regulation of the Rip1/Rip3 necrosome (36, 37). We provide evidence that, directly downstream of TLR4, macrophages deficient in either TRIF or Myd88 are capable of activating Rip1 phosphorylation but show significant differences in the phosphorylation of Rip3. Specifically, we show, for the first time to our knowledge, that TRIF acts specifically to induce a longer-lasting activation of Rip3. In general, our data indicate either that multiple kinases are likely able to activate Rip1 kinase or that a common pathway between these diverse receptors must activate Rip1. Furthermore the location, timing, and extent of Rip1 activation are likely determinants of the activation of Rip3 and downstream necroptotic cell death machinery.

We demonstrate that IFNAR1 signaling downstream of TRIF is responsible for the sustained activation of Rip3 kinase. In addition, we show that IFNAR1-deficient macrophages are resistant to TNF-α/zVAD–induced necroptosis, a surprising finding given that TNFR signaling has been studied so extensively as a direct activator of Rip1-dependent death (3). Consistent with such

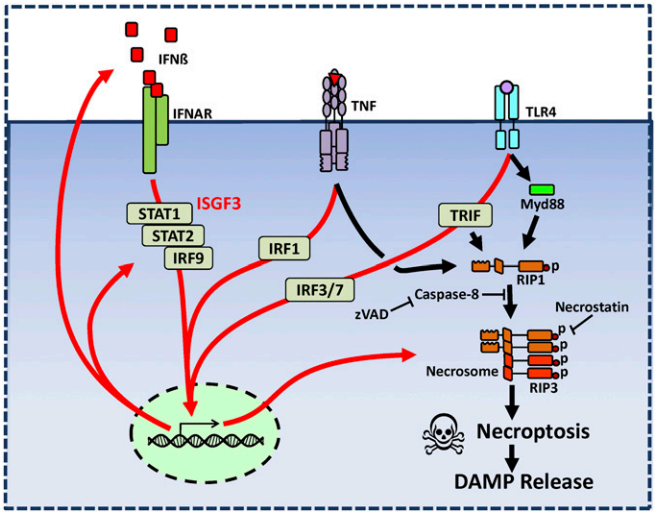

Fig. 7. Model of the role of IFN-I signaling as a key inducer of necroptosis. A number of cell-surface receptors lead to the activation of autocrine IFNAR1 signaling through redundant IRF family members. IFNAR1 signaling eventually leads to the assembly and activation of the ISGF3 complex, which in turn promotes sustained activation of the Rip1/Rip3 necrosome complex. Ultimately sustained necrosome activation leads to the induction of necroptotic cell death and release of inflammatory DAMPs.

a view, work has shown that IFNAR1-deficient mice are resistant to TNF-α–induced shock in vivo (27). Consistent with our observations, this pathway of TNF-α–induced IFN-β expression has been demonstrated to occur through an IRF-1–dependent mechanism (38) and appears to occur within endothelial cells as well as macrophages (39). Underlining the importance of IFNAR1, we also have observed that LPS- or polyI:C-induced necroptosis of macrophages is unaffected by the lack of TNFR1/2 but is highly dependent on IFNAR1 expression. Our results add IFN-I to a growing list of cellular signaling mechanisms, including multiple TLRs, death receptors, and cell stress pathways, known to activate Rip1 kinase (34, 40). Furthermore, our data show that, although TNFR expression is not specifically required for necroptosis to occur, IFN-I signaling appears to be required for necroptosis in macrophages.

To elucidate how IFNAR1 is able to support a sustained activation of the Rip1/Rip3 necrosome, we also examined a number of additional deficient mice. Consistent with previous understanding of IRFs (41), we found evidence of redundancy in the role of various IRFs in activating the expression and release of IFN-I in response to TLR stimulation. In contrast to our observations in other IRFs, IRF9-deficient macrophages phenocopied IFNAR1-deficient cells, exhibiting little necroptotic cell death in response to LPS, IFN-β, or TNF-α. In addition to IRF9, we find that STAT1- or STAT2-deficient macrophages are partially resistant to necroptosis, supporting a view that ISGF3 is required for late activation of Rip3 kinase. In contrast to previous work (42), we have excluded a role for PKR in the induction of IFNAR1-dependent necroptosis. Further work will be necessary to elucidate the exact mechanism by which IRF9/ISGF3 sustains the activation of Rip3 at later time points, but here we add to recent work showing that IRF9 specifically mediates the antiproliferative and proapoptotic effects of IFN-α (43).

The importance of necroptosis to the inflammatory program in vivo has become an intensive area of study in recent years. Studies have demonstrated that deficiency in Rip1/Rip3 signaling in vivo leads to less inflammatory pathology in various mouse models of systemic inflammatory shock (11–13). Similarly, work has directly implicated IFN-I signaling in systemic shock (25, 27). Despite the extensive use of zVAD as an inducer of necroptosis in vitro (28), only recently has it has been used as a means of investigating necroptosis in vivo (2). In our in vivo model, we used a combination of zVAD and LPS to study the effects of necroptotic cell death in vivo. Our results provide a mechanism by which IFN-I drives Rip3-dependent necroptotic cell death and in turn can drive inflammation through the release of inflammatory DAMPs such as high-mobility group box-1 (HMGB1) protein (10). Consistent with this proposed mechanism, elevated serum levels of HMGB1 are commonly seen in patients undergoing septic shock (44), and the blocking of HMGB1 is being pursued for therapeutic purposes (45).

In summary, the data presented in this article show that IFN-I signaling drives the sustained activation of the Rip1/Rip3 necrosome necessary for necroptosis of innate immune cells that ultimately leads to inflammatory pathology. This finding may illuminate new therapeutic avenues to intervene in cases of acute inflammatory pathology such as sepsis.

Experimental Procedures

Animal Work. Animals were maintained in accordance with Canadian Council on Animal Care guidelines. Protocols and procedures were approved and monitored by the National Research Council of Canada-Institute for Biological Sciences Animal Care and Ethics Board and/or the University of Ottawa Animal Care Committee. Strains of mice used for experiments are as follows: WT C57BL6/J (Jax #000664), TRIF$^{-/-}$ (Jax #005037), Myd88$^{-/-}$ (Jax #009088), TNFR1/2$^{-/-}$ (Jax #003243), IFNAR1$^{-/-}$ (a kind gift from Kaja Murali-Krishna, Emory University, Atlanta), and PKR-knockout mice and matched controls (obtained from John Bell, Ottawa Hospital Research Institute Ottawa) were on the 129SvEv background (46). STAT1$^{-/-}$ mice (Taconic 2045-F) and matched WT controls (Taconic 129SVE-F) were obtained from Taconic. STAT2$^{-/-}$ mice were generated by crossing 129SvJ/Stat2$^{-/-}$ mice (a kind gift from Christian Schindler, Columbia University, New York) onto the C57/BL6 background for 11 generations. Rip3$^{-/-}$ mice were a kind gift from Vishva Dixit (Genentech, San Francisco). IRF3$^{-/-}$ mice were generated as described in ref. 47; IRF7$^{-/-}$ mice were generated as described in ref. 19; IRF9$^{-/-}$ mice were generated as described in ref. 48; and IRF3/7$^{-/-}$ mice were generated as described in ref. 49. Genetic analysis necessary for strain determination was performed using tail clips and genomic PCR. Experiments using multiple transgenic mice used age- and sex-matched mice. Unless otherwise stated transgenic mice were on the C57BL6 genetic background.

In Vivo Endotoxin Shock Models. Mice were injected i.p. with differing amounts of LPS and/or zVAD as described in the text. Body temperature was monitored to assess animal health, and mice were killed at established humane endpoints (body temperature less than 27 °C). After mice were killed, peritoneal lavage was performed with 10 mL of cold PBS, and blood was drawn via cardiac puncture.

Generation of Macrophages and Mouse Embryonic Fibroblasts. Mouse bone marrow was differentiated for 7 d using macrophage colony-stimulating factor to generate macrophage cells. Primary mouse embryonic fibroblasts were prepared by standard procedures (50) and immortalized by E1A/Ras transformation (51).

In Vitro Cell Stimulations and Microscopy. Macrophages were treated with various PAMPs such as LPS (100 ng/mL) or poly I:C (20 μg/mL) or with cytokines such as TNF-α (50 ng/mL) or IFN-β (25 ng/mL) in the absence or presence of zVAD (25 or 50 μM). Cell death was quantitated at various time intervals after treatment.

For cell imaging, macrophages were plated in a 96-well flat-bottom plate at 7×10^4 cells per well 24 h before the addition of inhibitors and agonists. Cells were treated with corresponding reagents for 24 h, stained with Hoechst (2.5 μg/mL; Invitrogen, 33342) and propidium iodide (1:10 dilution; BD Pharmingen, 550825), and incubated at 37 °C for 25 min before being examined by immunofluorescence microscopy using a Zeiss AxioObserver.D1 microscope. The AxioVision Rel. 4.8 program was used to analyze images. Cells were quantitated using the Lumenera Infinity Analyze program.

In Vitro Inhibitor Assays. Macrophages were treated with a variety of small molecule inhibitors over the course of experiments as described in the text. Inhibitors used were as follows: z-VAD-FMK (EMD Millipore, 627610), LPS from *E. coli* 055:B5 (Sigma, L4005), Necrostatin-1 (Sigma, 9037), TNF-α (R&D Systems, 410-MT), mouse IFN-β (PBL InferonSource, Life Technologies, 12400-1), and polyI:C (Sigma-Aldrich, P1530). A variety of techniques were used for experiments; details are given in the text. In general, macrophages were given 24 h to adhere to the plates before treatment with inhibitors was initiated. After treatment with appropriate concentrations of inhibitors, cells were left for 24 h before cell death or viability was assessed, unless otherwise stated in the text. In experiments that used LPS stimulation, a concentration of 100 ng/mL was used consistently. Experiments to generate protein lysates from cells were performed with 250,000 cells per well in 24-well plates and were terminated at various time points.

Viability Assays (MTT Assay). Cell viability was assessed using the 3-[4,5-dimethylthiazol-2-yl]-2,5-diphenyltetrazolium bromide (MTT) assay. MTT staining reagent was added to cells at a final concentration of 0.5 mg/mL and incubated at 37 °C for 2 h. Then cells were lysed, and the MTT crystals were solubilized using 5 mM HCl in isopropyl alcohol. Results were quantified by measuring absorption at 570 nm with a reference wavelength of 650 nm on a Molecular Devices Emax plate reader. Viability measurements were normalized to the similarly stimulated control (i.e., LPS+zVAD normalized to LPS alone of the same genotype) unless otherwise described. Cell death also was assessed using a commercial lactate dehydrogenase release assay (Sigma-Aldrich, TOX7) according to the manufacturer's instructions.

Western Blotting. Cell lysates were obtained during various experiments by lysing cells directly in 1% SDS lysis buffer with 1% β-mercaptoethanol and boiling immediately to minimize protein degradation. (Note: We have found the phosphorylated forms of Rip1 and Rip3 are highly sensitive to the lysis buffer and protocol used.) Western blot analysis was performed by standard protocol. Antibodies used were as follows: mouse anti-Rip1 (BD, 610458), mouse anti-Rip3 (ProSci Inc., 2283), mouse anti-actin (BD, 612656), rabbit anti-STAT1 (Cell Signaling, 9172), rabbit anti-pSTAT1 (Cell Signaling, 9167), rabbit anti-STAT2 (Cell Signaling, 4597), and rat anti-MLKL monoclonal (EMD Millipore, MABC604). We confirmed the specificity of the Rip3 antibody used here by the absence of Rip3 signal in the Rip3-deficient

macrophages (Fig. S6). Our recent work with recombinant Rip1 also confirms the specificity of the Rip1 antibody used here (52).

FACS Cell Staining. Peritoneal cells were stained with antibodies against CD11b and F4/80 followed by staining with propidium iodide and were evaluated on a BD FACSCanto II Flow cytometer.

Cytokine Array. Serum cytokines were screened using the Multi-Analyte ELISArray Kit (SABiosciences, MEM-004A) according to the manufacturer's instructions. The absorbance values were read at 450 nm on a FilterMax F5 Multimode microplate reader (Molecular Devices). Wavelength correction was done by subtracting the readings at 570 nm. Cytokine concentrations were calculated in picograms per milliliter based on the OD values obtained for the standards.

Quantitative RT-PCR. Total RNA was isolated using TRIzol reagent (Life Technologies). Isolated RNA was reverse transcribed into cDNA in a 20-μL reaction volume using SuperScript III Reverse Transcriptase (Invitrogen,18080–044) as follows: 1 μg of RNA template was added to 0.5 μL of oligo(dT) (50 μM), 0.5 μL of random primers (50–250 ng), 4 μL of 5× First Strand buffer, 1 μL of DTT (0.1 M), 1 μL of dNTP (10 mM), 1 μL of RNase OUT (40 units/μL), and 1 μL of SuperScript III (200 units/μL). After cDNA synthesis, 2 μL of cDNA was analyzed using the SYBR Green (Life Technologies) fast method performed on an Applied Biosystems 7500 quantitative RT-PCR system. The primers used were as follows: Actin (forward) 5′-GATCAAGATCATTGCTCCTCCTG-3′, (reverse) 5′-AGGGTGTAAAACGCAGCTCA-3′; IRF-9 (forward) 5′-AGCAACTG CAACTCTGAGCTA-3′, (reverse) 5′-ACTCGGC CACCATA GATGAAG-3′.

Statistical Analyses. All graphs show the average result taken from at least three experiments, each performed in triplicate. Error bars show the SEM. Significance was determined by Student's *t* test using the GraphPad Prism software package.

ACKNOWLEDGMENTS. This work was funded by a grant from the Canadian Institutes of Health Research.

1. Akira S, Uematsu S, Takeuchi O (2006) Pathogen recognition and innate immunity. *Cell* 124(4):783–801.
2. He S, Liang Y, Shao F, Wang X (2011) Toll-like receptors activate programmed necrosis in macrophages through a receptor-interacting kinase-3-mediated pathway. *Proc Natl Acad Sci USA* 108(50):20054–20059.
3. Christofferson DE, Yuan J (2010) Necroptosis as an alternative form of programmed cell death. *Curr Opin Cell Biol* 22(2):263–268.
4. McComb S, et al. (2012) cIAP1 and cIAP2 limit macrophage necroptosis by inhibiting Rip1 and Rip3 activation. *Cell Death Differ* 19(11):1791–1801.
5. Upton JW, Kaiser WJ, Mocarski ES (2012) DAI/ZBP1/DLM-1 complexes with RIP3 to mediate virus-induced programmed necrosis that is targeted by murine cytomegalovirus vIRA. *Cell Host Microbe* 11(3):290–297.
6. Tenev T, et al. (2011) The Ripoptosome, a signaling platform that assembles in response to genotoxic stress and loss of IAPs. *Mol Cell* 43(3):432–448.
7. Wong WW-L, et al. (2014) cIAPs and XIAP regulate myelopoiesis through cytokine production in a RIPK1 and RIPK3 dependent manner. *Blood* 123(6):2562–72.
8. Ofengeim D, Yuan J (2013) Regulation of RIP1 kinase signalling at the crossroads of inflammation and cell death. *Nat Rev Mol Cell Biol* 14(11):727–736.
9. Christofferson DE, et al. (2012) A novel role for RIP1 kinase in mediating TNFα production. *Cell Death Dis* 3:e320.
10. Kaczmarek A, Vandenabeele P, Krysko DV (2013) Necroptosis: The release of damage-associated molecular patterns and its physiological relevance. *Immunity* 38(2):209–223.
11. Linkermann A, et al. (2012) Dichotomy between RIP1- and RIP3-mediated necroptosis in tumor necrosis factor-α-induced shock. *Mol Med* 18:577–586.
12. Duprez L, et al. (2011) RIP kinase-dependent necrosis drives lethal systemic inflammatory response syndrome. *Immunity* 35(6):908–918.
13. Takahashi N, et al. (2012) Necrostatin-1 analogues: Critical issues on the specificity, activity and in vivo use in experimental disease models. *Cell Death Dis* 3:e437.
14. Kawai T, Akira S (2006) TLR signaling. *Cell Death Differ* 13(5):816–825.
15. Baccala R, Hoebe K, Kono DH, Beutler B, Theofilopoulos AN (2007) TLR-dependent and TLR-independent pathways of type I interferon induction in systemic autoimmunity. *Nat Med* 13(5):543–551.
16. Kaiser WJ, et al. (2013) Toll-like receptor 3-mediated necrosis via TRIF, RIP3, and MLKL. *J Biol Chem* 288(43):31268–31279.
17. Hervas-Stubbs S, et al. (2011) Direct effects of type I interferons on cells of the immune system. *Clin Cancer Res* 17(9):2619–2627.
18. Sen GC, Sarkar SN (2007) The interferon-stimulated genes: Targets of direct signaling by interferons, double-stranded RNA, and viruses. *Curr Top Microbiol Immunol* 316:233–250.
19. Honda K, Taniguchi T (2006) IRFs: Master regulators of signalling by Toll-like receptors and cytosolic pattern-recognition receptors. *Nat Rev Immunol* 6(9):644–658.
20. Friedman RM (2008) Clinical uses of interferons. *Br J Clin Pharmacol* 65(2):158–162.
21. Kiladjian J-J, Mesa RA, Hoffman R (2011) The renaissance of interferon therapy for the treatment of myeloid malignancies. *Blood* 117(18):4706–4715.
22. Plosker GL (2011) Interferon-β-1b: A review of its use in multiple sclerosis. *CNS Drugs* 25(1):67–88.
23. Trinchieri G (2010) Type I interferon: Friend or foe? *J Exp Med* 207(10):2053–2063.
24. Li Q, et al. (2008) Interferon-α initiates type 1 diabetes in nonobese diabetic mice. *Proc Natl Acad Sci USA* 105(34):12439–12444.
25. Kelly-Scumpia KM, et al. (2010) Type I interferon signaling in hematopoietic cells is required for survival in mouse polymicrobial sepsis by regulating CXCL10. *J Exp Med* 207(2):319–326.
26. Mahieu T, et al. (2006) The wild-derived inbred mouse strain SPRET/Ei is resistant to LPS and defective in IFN-beta production. *Proc Natl Acad Sci USA* 103(7):2292–2297.
27. Huys L, et al. (2009) Type I interferon drives tumor necrosis factor-induced lethal shock. *J Exp Med* 206(9):1873–1882.
28. Degterev A, et al. (2005) Chemical inhibitor of nonapoptotic cell death with therapeutic potential for ischemic brain injury. *Nat Chem Biol* 1(2):112–119.
29. Galluzzi L, Kroemer G (2008) Necroptosis: A specialized pathway of programmed necrosis. *Cell* 135(7):1161–1163.
30. Robinson N, et al. (2012) Type I interferon induces necroptosis in macrophages during infection with Salmonella enterica serovar Typhimurium. *Nat Immunol* 13(10):954–962.
31. Taniguchi T, Ogasawara K, Takaoka A, Tanaka N (2001) IRF family of transcription factors as regulators of host defense. *Annu Rev Immunol* 19:623–655.
32. Gough DJ, Messina NL, Clarke CJP, Johnstone RW, Levy DE (2012) Constitutive type I interferon modulates homeostatic balance through tonic signaling. *Immunity* 36(2):166–174.
33. Mahieu T, Libert C (2007) Should we inhibit type I interferons in sepsis? *Infect Immun* 75(1):22–29.
34. Vanlangenakker N, Vanden Berghe T, Vandenabeele P (2012) Many stimuli pull the necrotic trigger, an overview. *Cell Death Differ* 19(1):75–86.
35. Cho YS, et al. (2009) Phosphorylation-driven assembly of the RIP1-RIP3 complex regulates programmed necrosis and virus-induced inflammation. *Cell* 137(6):1112–1123.
36. Lin Y, Devin A, Rodriguez Y, Liu ZG (1999) Cleavage of the death domain kinase RIP by caspase-8 prompts TNF-induced apoptosis. *Genes Dev* 13(19):2514–2526.
37. Oberst A, et al. (2011) Catalytic activity of the caspase-8-FLIP(L) complex inhibits RIPK3-dependent necrosis. *Nature* 471(7338):363–367.
38. Yarilina A, Park-Min K-H, Antoniv T, Hu X, Ivashkiv LB (2008) TNF activates an IRF1-dependent autocrine loop leading to sustained expression of chemokines and STAT1-dependent type I interferon-response genes. *Nat Immunol* 9(4):378–387.
39. Venkatesh D, et al. (2013) Endothelial TNF receptor 2 induces IRF1 transcription factor-dependent interferon-β autocrine signaling to promote monocyte recruitment. *Immunity* 38(5):1025–1037.
40. Meylan E, Tschopp J (2005) The RIP kinases: Crucial integrators of cellular stress. *Trends Biochem Sci* 30(3):151–159.
41. Schmid S, Mordstein M, Kochs G, García-Sastre A, Tenoever BR (2010) Transcription factor redundancy ensures induction of the antiviral state. *J Biol Chem* 285(53):42013–42022.
42. Thapa RJ, et al. (2013) Interferon-induced RIP1/RIP3-mediated necrosis requires PKR and is licensed by FADD and caspases. *Proc Natl Acad Sci USA* 110(33):E3109–E3118.
43. Tsuno T, et al. (2009) IRF9 is a key factor for eliciting the antiproliferative activity of IFN-alpha. *J Immunother* 32(8):803–816.
44. Sundén-Cullberg J, et al. (2005) Persistent elevation of high mobility group box-1 protein (HMGB1) in patients with severe sepsis and septic shock. *Crit Care Med* 33(3):564–573.
45. Lamkanfi M, et al. (2010) Inflammasome-dependent release of the alarmin HMGB1 in endotoxemia. *J Immunol* 185(7):4385–4392.
46. Zhu PJ, et al. (2011) Suppression of PKR promotes network excitability and enhanced cognition by interferon-γ-mediated disinhibition. *Cell* 147(6):1384–1396.
47. Sato M, et al. (2000) Distinct and essential roles of transcription factors IRF-3 and IRF-7 in response to viruses for IFN-alpha/beta gene induction. *Immunity* 13(4):539–548.
48. Kimura T, et al. (1996) Essential and non-redundant roles of p48 (ISGF3 gamma) and IRF-1 in both type I and type II interferon responses, as revealed by gene targeting studies. *Genes Cells* 1(1):115–124.
49. Daffis S, Suthar MS, Szretter KJ, Gale M, Jr, Diamond MS (2009) Induction of IFN-beta and the innate antiviral response in myeloid cells occurs through an IPS-1-dependent signal that does not require IRF-3 and IRF-7. *PLoS Pathog* 5(10):e1000607.
50. Xu, J (2005) Preparation, culture and immortalization of mouse embryonic fibroblasts. *Curr Protoc Mol Biol* 28(Suppl 70):28.1.1–28.1.8.
51. Serrano M, Lin AW, McCurrach ME, Beach D, Lowe SW (1997) Oncogenic ras provokes premature cell senescence associated with accumulation of p53 and p16INK4a. *Cell* 88:593–602.
52. McComb S, et al. (2014) Cathepsins Limit Macrophage Necroptosis through Cleavage of Rip1 Kinase. *J Immunol* 192(12):5671–5678.